Fall Technical Meeting of the Eastern States Section of the Combustion Institute
Hosted by the University of Connecticut, Storrs, CT
Oct 9-12, 2011

Laminar Flame Speeds of Cyclohexane and Mono-alkylated Cyclohexanes at Elevated Pressures

Fujia Wu, Andrew P. Kelley and Chung K. Law

Department of Mechanical and Aerospace Engineering, Princeton University, Princeton, New Jersey 08544, USA

Laminar flame speeds of cyclohexane, methyl-cyclohexane and ethyl-cyclohexane at atmospheric and elevated pressures up to 20 atm were determined in a heated, dual-chamber vessel using nonlinear extrapolation. Calculated values using JetSurf 2.0 mechanism yielded satisfactory agreement with the present measurements at all pressures, with slight over-prediction at 1 atm. Results show that the flame speeds of methyl-cyclohexane and ethyl-cyclohexane are similar, while those of cyclohexane are higher by 5% at 1 atm and 13% at 10 atm. Examination of computed flame structure shows that owing to its special, symmetric ring structure, cyclohexane produces substantially more chain-branching C_2 and C_4 intermediates than the relatively less reactive C_3 intermediates. On the contrary, a more balanced distribution of C_2-C_4 intermediates is present in flames of methyl- and ethyl-cyclohexane due to the substitution of alkyl group for H.

1. Introduction

Cyclo-alkanes are components of commercial fuels, and their concentrations become more substantial in alternative fuels, particularly those derived from coal [1-3]. However, their combustion characteristics and oxidation kinetics have not been studied as extensively as n-alkanes.

There have been relatively few measurements of laminar flame speeds for cyclo-alkanes, and most data were obtained at atmospheric pressure or slightly elevated pressures. Davis & Law [4] measured the laminar flame speeds for cyclohexane and cyclopentane at atmospheric pressure and unburned gas temperature of 298 K; Farrell *et al.*[5] for cyclohexane, cyclopentane, and methyl-cyclopentane at 3 atm and 450 K; Dubois *et al.* [6] for n-propyl-cyclohexane at 403 K and atmospheric pressure; and Ji *et al.* [7] for cyclohexane, methyl-, ethyl-, n-propyl- and n-butyl-cyclohexane at 353 K and atmospheric pressure.

As representative cyclo-alkanes, cyclohexane and its mono-alkylated derivatives have been selected as components of surrogate gasoline [1], diesel [2] and jet fuel [3]. Recently, a detailed chemical reaction model, the Jet Surrogate Fuel (JetSurf) [8], with the newest version being 2.0, has been developed for the combustion of jet fuel surrogate. The performance of JetSurf 2.0 in predicting laminar flame speeds of cyclohexane and mono-alkylated cyclohexanes has been well validated at atmospheric pressure in Ref. [7]; however, its performance at elevated pressures has not been evaluated.

The fundamental understanding on the decomposition and further oxidation of cyclo-alkanes is also of interest. Studies of the laminar flame speeds of C_5-C_8 [9] alkanes showed that they are

almost identical. The reason for this fuel similarity has been attributed [9-11] to the fact that n-alkanes all crack into similar small fragments (C_0-C_4) in flames due to their similar straight chain molecular structure. However, this fuel similarity does not seem to exist for cyclo-alkanes in the measurements of Ji *et al.* [7]. It was found that the flame speeds of mono-alkylated cyclohexanes from methyl- to n-butyl- were nearly identical but that of cyclohexane was higher by roughly 7-8%. Realizing that the adiabatic flame temperature between these fuels are very close, Ji *et al.* [7] attributed the difference in their flame speeds to chemical kinetic effect, caused by the change in the distribution of smaller molecules formed when the original fuel molecules decompose as they approach the active reaction zone. Mono-alkylated cyclohexane was found to produce allyl and propene while cyclohexane more 1,3-butadiene. The allyl and propene species then lead to chain terminating reactions while 1,3-butadiene would lead to chain branching, resulting in a lower flame speed for the mono-alkylated cyclohexanes as opposed to cyclohexane.

The present study aims to provide archival laminar flame speed data for cyclohexane, methyl- and ethyl-cyclohexane at pressures from 1 atm to 20 atm at the initial temperature of 353 K. These measurements will allow us to investigate the pressure effect on the flame propagation of cyclohexane and its mono-alkylated derivatives; for instance whether the effect of alkyl substitution on laminar flame speed still holds at elevated pressures. Furthermore, substantial data at various conditions also allow for further understanding of the thermal decomposition and oxidation of cyclo-alkanes.

2. Experimental Specifications

2.1 Experimental setup

Laminar flame speeds were determined using expanding spherical flames. Detailed descriptions and dimensions of the experimental apparatus, procedure and data analysis were reported in two previous publications [9,12]. Here we therefore provide only a brief description of the experimental apparatus and procedure.

The apparatus modifies the previous dual-chamber design for spherical flames to allow experimentation with liquid fuels at elevated temperatures. It consists of a cylindrical chamber radially situated within an outer chamber of substantially larger volume. The wall of the inner chamber is fitted with a series of holes that can be mechanically opened and closed to allow the union and separation of the gases in the inner and outer chambers. The outer chamber is covered with silicon electrical heaters, hence enabling it to act as an oven to uniformly heat the inner chamber to 353 K, which is the initial gas temperature for all of the present data.

The experimental procedure involves first filling the inner chamber with fuel vapor produced by heating a fuel reservoir maintained at 353 K, followed by a certified mixture of oxidizer and inert gas which is also preheated to at least 353 K. The outer chamber is filled with a mixture of inert gases to match the density of the gas in the inner chamber. As a secondary check, samples of the gas in the tubing connected to the inner chamber are analyzed using a gas chromatograph with a flame ionization detector. All gas samples were verified to have less than a 2% random error in the equivalence ratio, as is expected based on the gas filling procedure.

Concurrent to the instant that the test gas in the inner chamber is spark ignited, the holes between the inner and outer chambers are opened, resulting in an expanding spherical flame that

propagates throughout the inner chamber in essentially an isobaric environment before it is quenched upon contacting the inert gases of the outer chamber. The flame surface is visualized using a pin-hole Schlieren system coupled to a high-speed camera running typically at 10,000 frames per second.

2.2 Data analysis

Tracking the flamefront yields the history of the radius of the spherical flame as a function of time, $r_f(t)$. For the extrapolation of the laminar flame speed from $r_f(t)$, we employed the relation recently derived by Kelly *et al.* [13] using asymptotic analysis,

$$S_b^0 t + C = r_f + 2L_b \ln r_f - \frac{4L_b^{\,2}}{r_f} - \frac{8L_b^{\,3}}{3r_f^{\,2}} \qquad (1)$$

where S_b^0 is the adiabatic, unstretched gas speed of the burned mixture relative to the flame, r_f the flame radius, L_b the Markstein length and t the time. It is noted that Equation (1) contains up to the third-order accuracy in terms of the inverse flame radius. Other extrapolation relations, such as the linear model [14], nonlinear model with quasi-steady approximation [15] and the Markstein's empirical equation [16] only contain up to first or second order accuracy. While the flame speeds extrapolated from the linear model are generally higher than that from the quasi-steady nonlinear model, for both $Le > 1$ and $Le < 1$ cases, using Equation (1) leads to results between the two but closer to the results using quasi-steady nonlinear model [15]. For typical hydrocarbon fuels, using Equation (1) and the quasi-steady nonlinear relation [15] causes a maximum difference of only approximately 1 cm/sec, with the difference increasing as the equivalence ratio deviates from 1.3, which typically corresponds to zero Markstein number.

For flame speed measurements using expanding spherical flames, the data selected for extrapolation need to be in a certain radius range in that the small and large radius data are respectively contaminated by the influences of ignition and the chamber confinement, which has been discussed in details in Refs [17-20]. For our experimental setup and the choice of fuel studied, a conservative assessment of this range is between radii of 1.0 to 1.8 cm. The actual selected data for extrapolation at each data point was within this range, assisted by assessment of the trajectories of dr_f/dt versus stretch rate, $(2/r_f)dr_f/dt$. Based on repeated measurements and the sensitivity of slight variation of the data selection, all reported laminar flame speeds in this paper have an uncertainty of approximate ± 2 cm/sec.

2.3 Numerical approach

For quantitative comparison and mechanism studies, numerical computation was performed using the Chemkin Premix code [21] to determine the laminar flame speeds as well as the reaction rate and species profiles. All calculations used multi-component formulation for transport properties and included Soret diffusion. The calculation used finite difference method with adaptive gridding, which was refined to the level where the two grid controlling parameters GRAD and CURV were both 0.05.

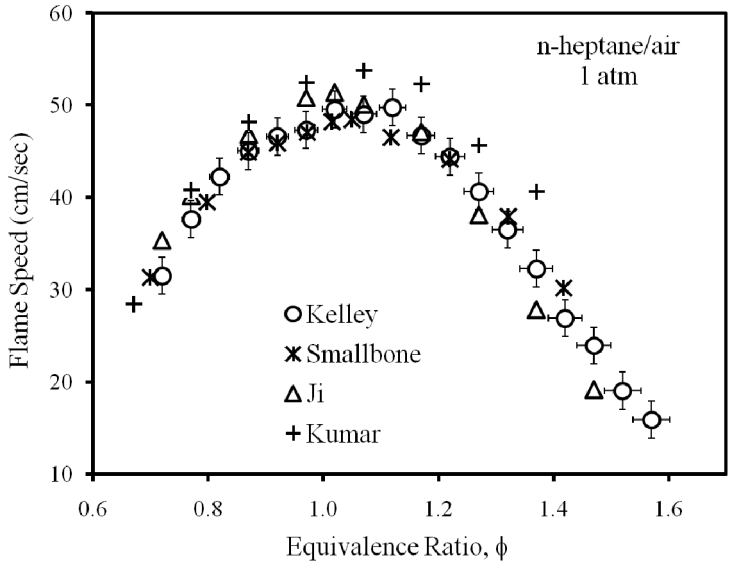

Figure 1: Comparison of laminar flame speeds of n-heptane/air at atmospheric pressures. Data include: Kelly et al. [9] (T_u = 353 K), Smallbone et al. [22] **(T_u = 350 K), Ji et al. [10] (T_u = 353 K) and Kumar et al.** [23] **(T_u = 360 K). A correction $S_u^o \sim T_u^{1.8}$ suggested by numerical predictions with JetSurf 2.0 mechanism was employed on measurements of Smallbone et al.** [22] **and Kumar et al.** [23] **to account for the small difference in the initial temperatures from 353 K.**

3. Results

3.1 Validation of Present Approach

In order to assess the validity of the present approach, we shall first compare the laminar flame speeds with those in the literature. For n-heptane at atmospheric pressure, which has been extensively studied in the literature, four independent measurements can be used for comparison: the data of Kelley *et al.* [9] obtained using the present experimental set-up, and the counterflow data of Ji *et al.* [10], Smallbone et al. [22] and Kumar *et al*. [23]. The data of Kelley *et al.* [9] has been re-analyzed using Equation (1) for extrapolation. The resulting comparison is plotted in Figure 1. It is seen that except for the data of Kumar et al. [23] which show consistently higher values, the other three measurements are in relatively close agreement. The difference between the measurements of Kelley *et al.* [9] and Smallbone et al. [22] are the smallest in spite of the difference in the experimental approaches. There is a slightly "lean-shift" between measurements of Ji *et al.* [10] and Kelley *et al.* [9]: the former peaks at $\phi \approx 1.05$ while the latter at $\phi \approx 1.1$. This discrepancy, although small, is out of the range of the experimental error and has consistently appeared in the data for other liquid fuels reported by the two groups. The source of this disagreement is yet to be determined. Furthermore, based on the present comparison as well as those in the literature, the data of Kumar *et al.* [23] appear to carry substantial though unquantified error, and as such may need to be excluded in future comparisons.

3.2 Results with air as oxidizer

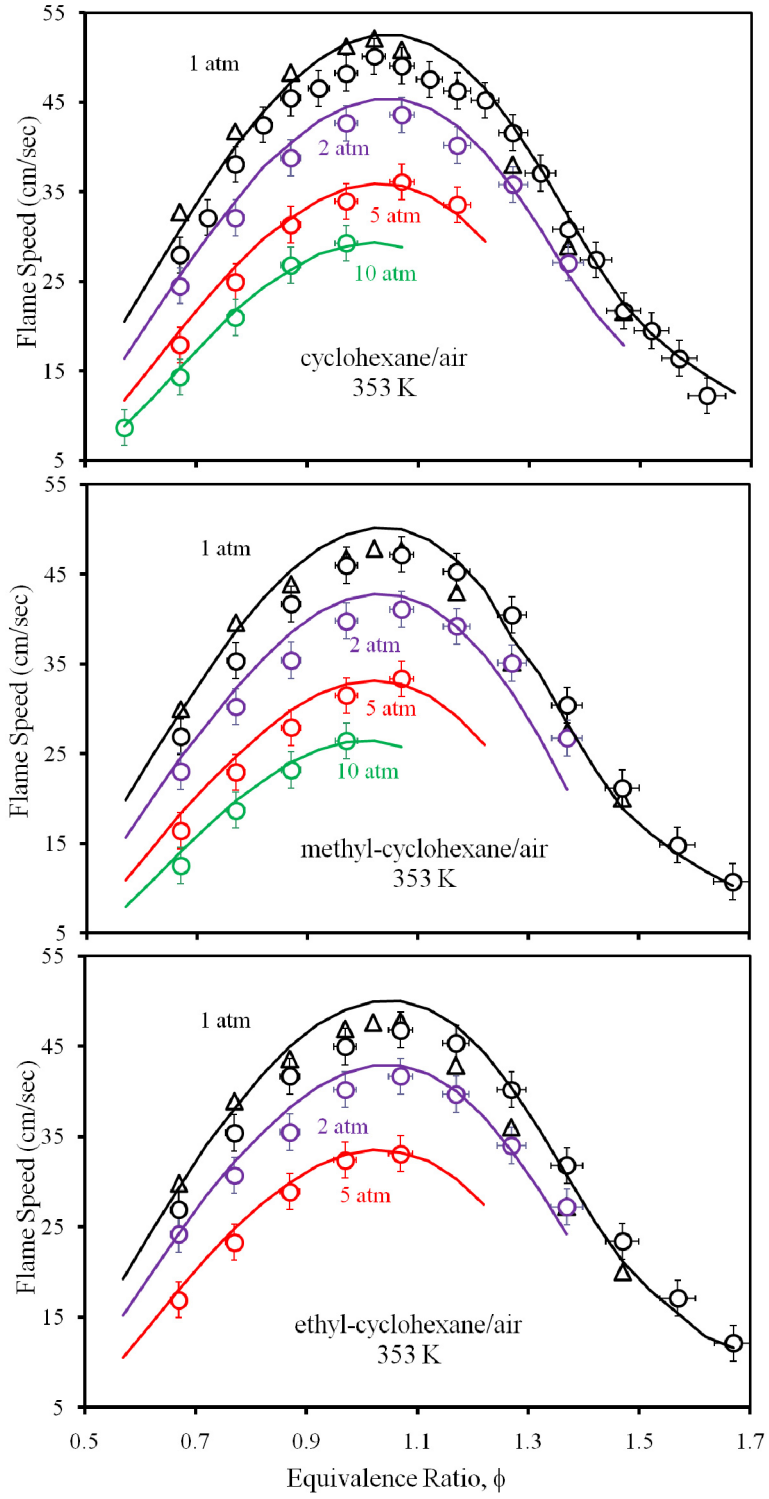

Figure 2: Laminar flame speeds of cyclohexane, methyl-cyclohexane and ethyl-cyclohexane at various pressures with air as the oxidizer, unburned gas temperature of 353 K. Cycles: present measurements; Triangles: measurements of Ji *et al.* [7]; Solid lines: computed values using JetSurf 2.0 mechanism (Wang *et al.* [8])

We shall next present the results using air from a certified cylinder of 21 mol% O_2/79 mol% N_2 as the oxidizer. The complete sets of data on the laminar flame speeds of cyclohexane, methyl-cyclohexane and ethyl-cyclohexane are shown in Figure 2, for pressures of 1, 2, 5, and 10 atm except for ethyl-cyclohexane for which saturation begins at 10 atm. For each pressure, the lean limit was such that the ignition energy available was not able to drive the flame beyond the critical radius required for successful flame initiation [17]. The rich limit for atmospheric pressure experiments was due to the onset of buoyancy effects when the flame speed is substantially reduced, while those at higher pressures were due to the onset of flamefront cellular instability.

Experimental data of Ji *et al.* [7] as well as the corresponding predictions of the JetSurF 2.0 mechanism [8] are also plotted in Figures 2 for comparison. Comparing the present measurements to those of Ji *et al.* [7], we see generally close agreement. However, the slight "lean-shift" in the peak location of flame speed is again observed: data of Ji *et al.* [7] tend to be slightly higher on the lean side and slightly lower on the rich side. Similar "lean-shift" is found in the comparison between measurements published from the two groups in Ref. [9] and [10] for the laminar flame speeds of n-alkanes.

In comparison with the chemical kinetic predictions of JetSurF 2.0 [8], it is seen that among all pressures the largest disagreement turns out to be at atmospheric pressure. The mechanism generally agrees quite well at elevated pressures with difference less than 3%. However, at atmospheric pressure there is a maximum difference of 6%, 8% and 7% for cyclohexane, methyl- and ethyl- cyclohexane, respectively. The peak values in the flame speeds are over-predicted for all three fuels, and there is also a slight shift in the peak locations to the lean side. Nevertheless, this overall agreement between measurements and model predictions at all pressures demonstrates the adequate performance of the mechanism in predicting the laminar flame speeds.

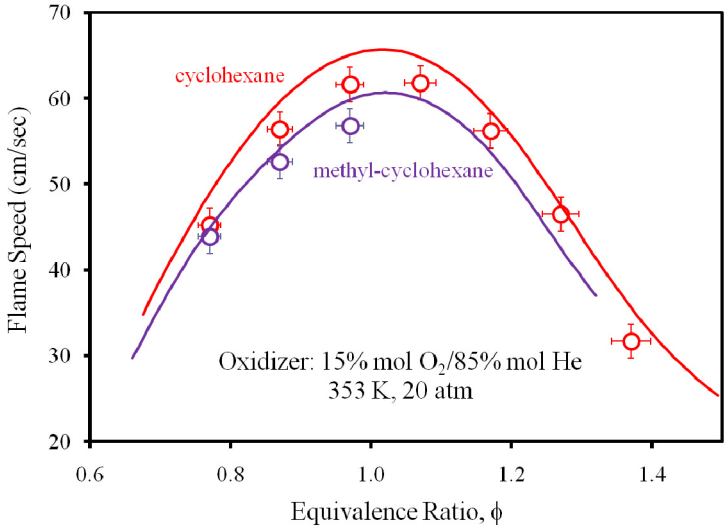

Figure 3: Laminar flame speeds of cyclohexane, methyl-cyclohexane with O_2/He mixture (15:85) as the oxidizer, at 20 atm unburned gas temperature of 353 K. Solid lines: computed values using JetSurf 2.0 mechanism (Wang *et al.* [8])

3.3 Results with oxygen/helium as oxidizer

In order to measure flame speeds at pressures higher than 10 atm, a mixture of 15 mol% O_2 with 85 mol% He was used in place of air. The use of helium in place of nitrogen results in a larger Lewis number for the mixture such that diffusional-thermal instabilities are more readily suppressed [20]. Additionally, decreasing the oxygen concentration results in an increase in the flame thickness. This tends to suppress the hydrodynamic instability which becomes progressively more prominent with increasing pressure.

The laminar flame speeds of cyclohexane and methyl-cyclohexane at 20 atm are plotted in Figure 3, along with the corresponding predictions by JetSurf 2.0 [8]. The absence of data for methyl-cylcohexane on the rich side and ethyl-cyclohexane was due to fuel vapor saturation at those conditions. Although with reduced oxygen concentration, the laminar flame speeds at 20 atm are much higher than those with air as the oxidizer at 10 atm due to the low specific heat and high conductivity of helium.

Comparing the present measurements to the predictions of JetSurF 2.0 [8], it is seen that the mechanism generally agrees quite well for methyl-cyclohexane, with maximum difference being less than 3%. However, for cyclohexane a slight over-prediction is seen uniformly, with a maximum difference of 6%, which is higher than the difference between measurements and predictions at 10 atm with air as the oxidizer.

4. Comparison and discussion for different fuels

4.1 Comparison of flame speeds

Experimental laminar flame speeds of cyclohexane, methyl- and ethyl-hexanes with air as the oxidizer are compared in Figure 4. The comparison of cyclohexane and methyl-cyclohexane with O_2/He as the oxidizer are shown in Figure 3. From the comparison it is seen that the laminar flame speeds of cyclohexane are uniformly higher than methyl- and ethyl-cyclohexane, and those of methyl- and ethyl-cyclohexane are almost identical. This result agrees with the trends found by Ji *et al.* [7] at atmospheric pressure. Furthermore, the present measurements show that the same trend can be extended to elevated pressures.

Numerical predictions of the laminar flame speeds for the three fuels by JetSurf 2.0 mechanism are compared in Figure 5. It is seen that the predictions well capture the same trend found in the experimental measurements. This means that the underlying mechanism responsible for the difference in the flame speeds between cyclohexane and its alkylated counterparts is possibly contained in the mechanism.

To identify the pressure effects more clearly, we plot the percentage difference in the maximum flame speed between the three fuels for both experimental and prediction data in Figure 6. It is seen that for the results with air as oxidizer, the difference between the flame speeds of cyclohexane and those of methyl- and ethyl-cyclohexane becomes larger as the pressure increases. The percentage difference increases from about 5% to roughly 13% as the pressure increase from 1 to 10 atm. The numerical predictions also show approximately the same extent of increase with pressure. For the results at 20 atm with O_2/He mixture as oxidizer, the difference decreases slightly from 10 atm, but it is still higher than the difference at atmospheric pressure.

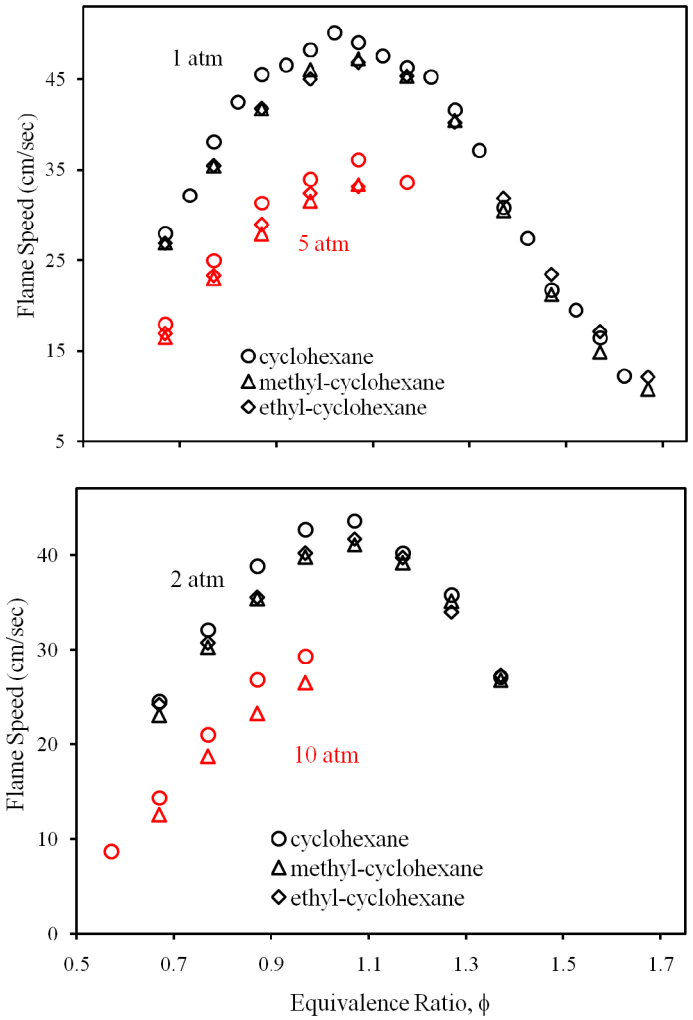

Figure 4: Comparison of measured laminar flame speeds of cyclohexane, methyl-cyclohexane and ethyl-cyclohexane at 1, 2, 5 and 10 atm with air as oxidizer

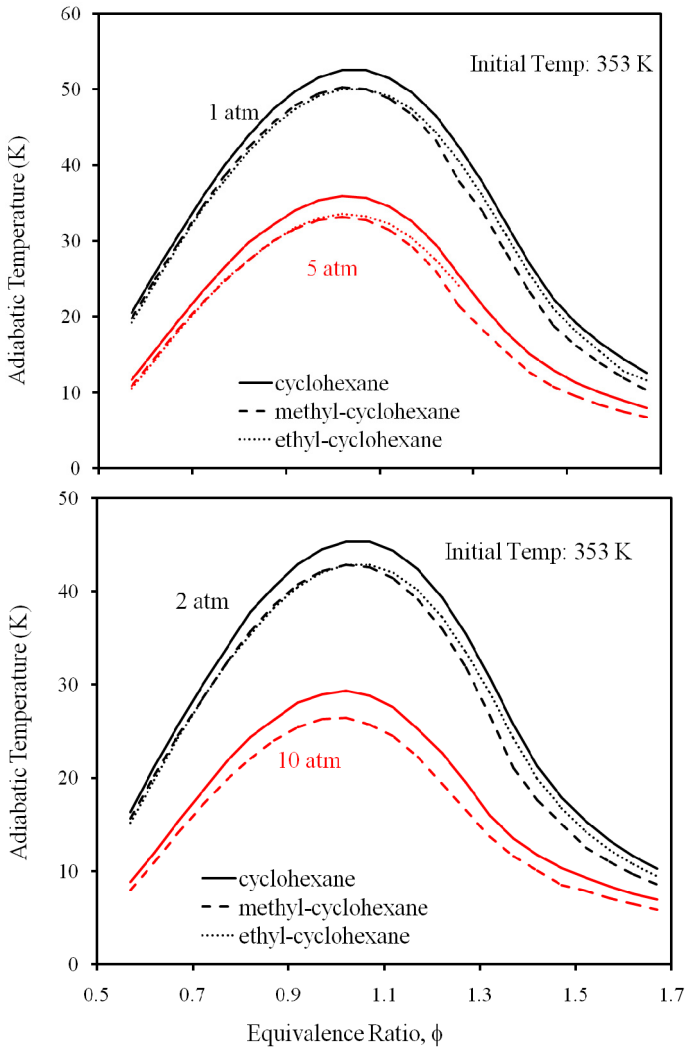

Figure 5: Comparison of predicted laminar flame speeds of cyclohexane, methyl-cyclohexane and ethyl-cyclohexane by JetSurf 2.0 mechanism (Wang *et al.* [8]) at 1, 2, 5 and 10 atm with air as oxidizer

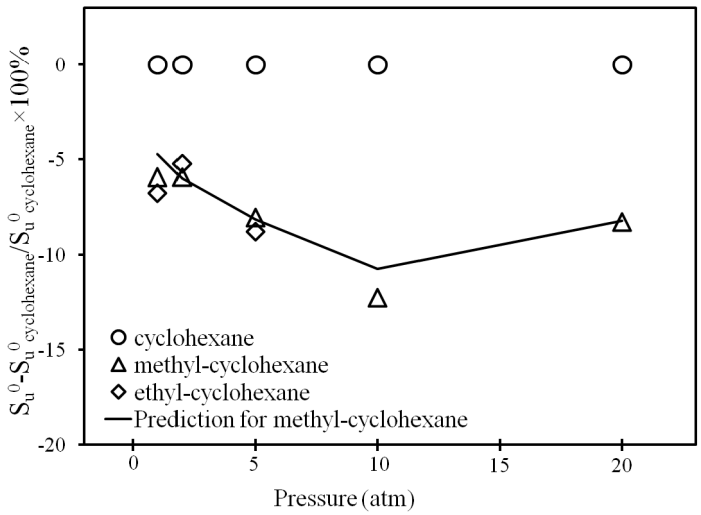

Figure 6: Percentage difference in maximum flame speed between cyclohexane, methyl- and ethyl-cyclohexane at various pressures. Measurements at 1, 2, 5, and 10 atm used air as oxidizer while those at 20 atm used O_2/He mixture (15:85) as the oxidizer.

4.2 Comparison of flame structure

The present measurements, those of Ji *et al.* [7], and the predictions by JetSurf 2.0 mechanism Wang *et al.* [8] all consistently show that substitution of methyl or ethyl for H in cyclohexane reduces the laminar flame speed, and the effect becomes more prominent as pressure increases. This result behooves us to seek the fundamental reasons.

We first note that the cause is not of thermal nature because all three fuels have almost the same adiabatic flame temperature, as shown in Figure 7 for their mixtures with air at atmospheric pressure. The maximum difference in the adiabatic flame temperature is less than 2 K. The adiabatic flame temperatures at elevated pressures are also nearly the same from the calculations. The difference in transport properties is also not considered as an important factor, because the molecular weights of the three fuels are similar to those of C_6-C_8 n-alkanes, for which similar flame speeds have been found [9].

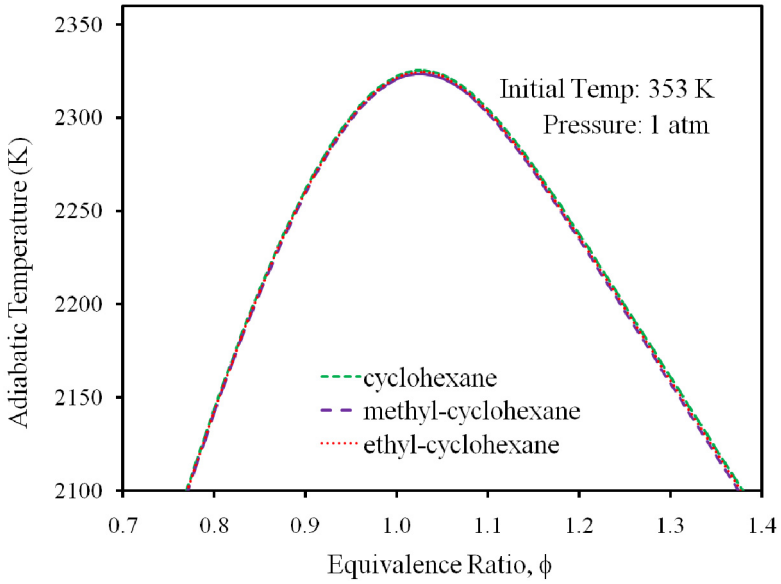

Figure 7: Comparison of adiabatic flame temperatures of n-hexane, cyclohexane, methyl- and ethyl-cyclohexanes at atmospheric pressure. Thermodynamic data in JetSurf 2.0 mechanism was used in the calculation.

We shall next examine the kinetic reasons. Figure 8 plots the temperature and heat release profiles for cyclohexane, methyl- and ethyl-cyclohexane for 1-D premixed flames obtained by JetSurf 2.0 mechanism at various pressures and for ϕ = 1.0. It is seen that the temperature profiles overlap at upstream and downstream boundaries but diverge in the middle, at which the temperature profile for cyclohexane is steeper than that of its alkylated derivatives, corresponding to an earlier and stronger heat release rate for cyclohexane. Furthermore, as pressure increases the heat release rate of cyclohexane is further increased and advanced, compared to methyl- and ethyl-cyclohexane. The maximum difference between the three fuels in peak heat release rate increases from 3% at 1 atm to 8% at 10 atm.

With the adiabatic flame temperature being the same, this difference in heat release clearly indicates a kinetic difference. In several previous work on the premixed flame structure of large-molecule fuels [7,9-11], it was suggested that the initial fuel cracking process to form small fuel fragment such as (CH_4, C_2H_4, *etc.*) and the oxidation of these fuel fragments can be decoupled. Furthermore, since the initial fuel cracking occurs relatively fast at temperatures above 1100 K, the oxidation of the fuel fragments mainly controls the heat release and eventually flame propagation.

Following this concept, we plot in Figure 10 the profiles of the major fuel fragments in flames of cyclohexane and methyl-cyclohexane flames at various pressures. It is seen that while the profiles of CH_4 and C_2H_6 are similar, there are considerably more C_3H_6, but less C_2H_4 and 1,3-C_4H_6 in flames of methyl-cyclohexane than those of cyclohexane. Considering that all other fuel

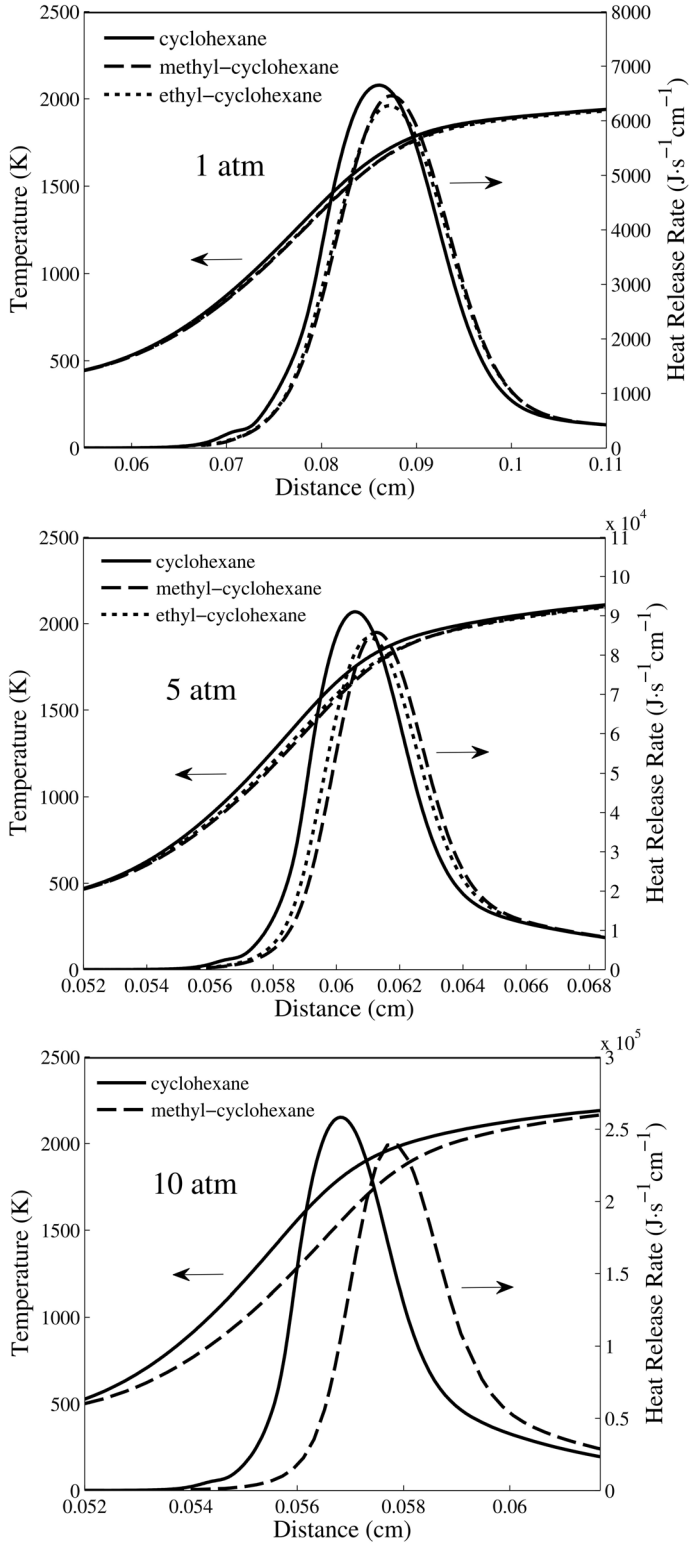

Figure 8: Temperature and heat release profiles for cyclohexane, methyl- and ethyl-cyclohexane 1-D flames with air calculated with JetSurF 2.0, ϕ = 1.0, unburned gas temperature of 353 K. The horizontal axis scales are zoomed according to flame thickness, with zero fixed at *T* = 400 K.

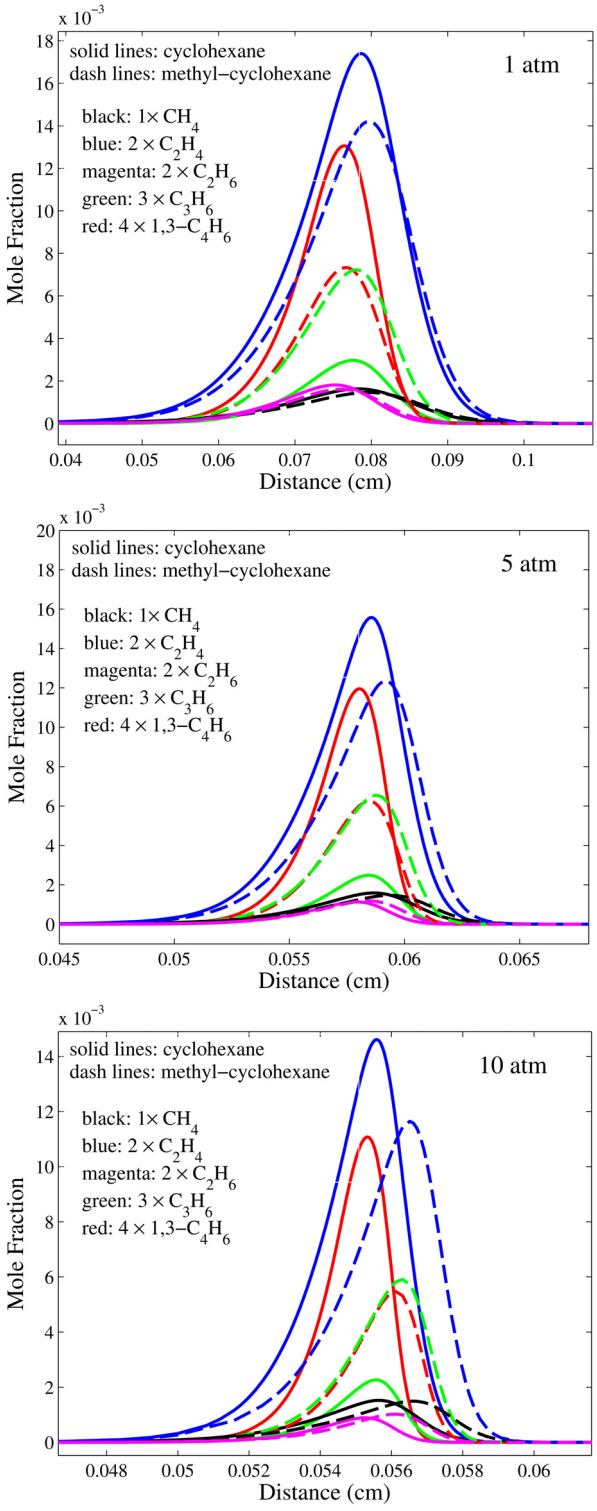

Figure 9: Profiles of major fuel fragments in 1-D flames of cyclohexane, methyl-cyclohexane calculated with JetSurF 2.0, ϕ = 1.0, unburned gas temperature of 353 K. The horizontal axis scales are zoomed proportional to flame thickness at different pressures.

fragments either have similar profiles for the two fuels or have low fractions (which means they are not rate-limiting species), it is possible that the difference in C_2H_4, C_3H_6 and 1,3-C_4H_6 distribution is the primary reason responsible for the observed difference in flame speeds. C_2H_6 has notably high reactivity and high flame speeds seen in many previous measurements [4,24,25]. The relatively low reactivity of C_3H_6 and high reactivity of 1,3-C_4H_6 were noted in Ref. [7]: the abstraction of H from C_3H_6 through reaction $C_3H_6+H\rightarrow aC_3H_5+H_2$ leads to aC_3H_5; however, aC_3H_5 tends to have recombination reaction through $aC_3H_5+H+M\rightarrow C_3H_6+M$ to regenerate C_3H_6, leading to secondary chain termination by forming a net sink for H. On the contrary, typical subsequent reactions of 1,3-C_4H_6 is to break the single C-C bond, for example, $1,3\text{-}C_4H_6+H\rightarrow C_2H_4+C_2H_3$, the products of which also have high reactivity.

The difference in kinetic behaviors among fuel fragments also explains the pressure effect seen in the heat release profiles and laminar flame speeds. Since increasing pressure leads to more third body reactions, it therefore aggravates the effects of fuel fragments that can lead to chain termination. For example, considering the reactions $aC_3H_5+H+M\rightarrow C_3H_6+M$ and $aC_3H_5+H\rightarrow aC_3H_4+H_2$ for example, calculation with JetSurf 2.0 mechanism shows that the ratio of the maximum reaction rates of the two reactions increases from 7.2 at 1 atm, to 8.1 at 5 atm, and 8.5 at 10 atm.

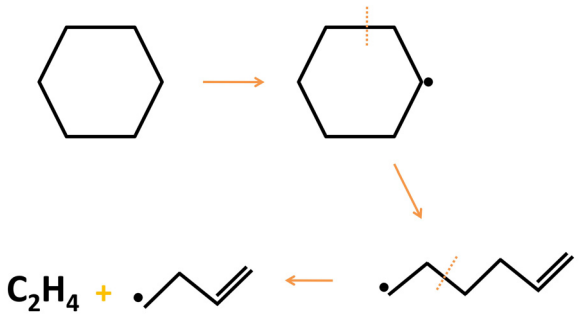

Figure 10: Initial ring opening and fuel cracking of cyclohexane at high temperature under the rule of b-Scission

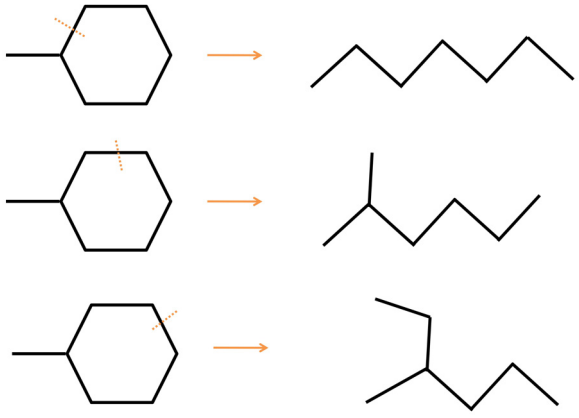

Figure 11: Impact of ring opening position of methyl-cyclohexane on molecular structure of subsequent species (position of radical site and double bond are not shown)

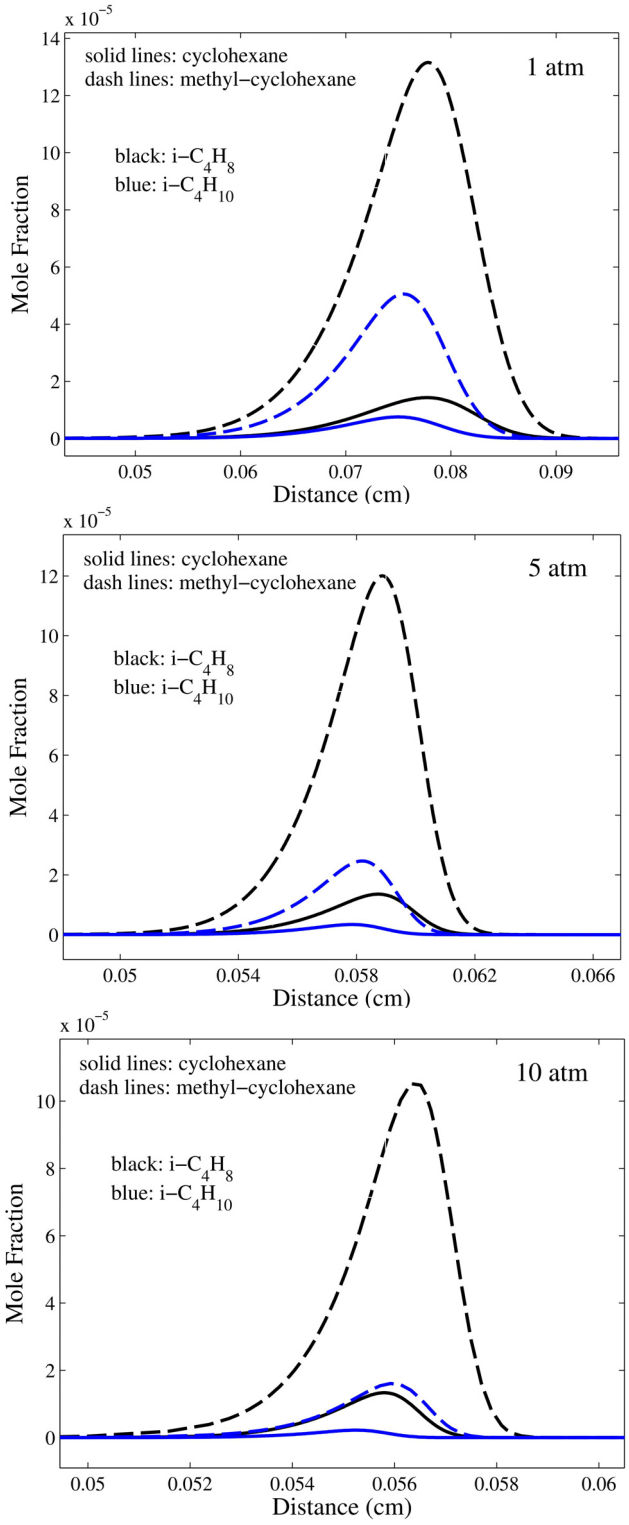

Figure 12: Profiles of iso-butane and iso-butene in 1-D flame of cyclohexane, methyl-cyclohexane calculated with JetSurF 2.0, ϕ = 1.0, unburned gas temperature of 353 K. The horizontal axis scales are zoomed proportional to flame thickness at different pressures.

4.3 Effect of alkyl-substitution

We shall next discuss the reason why the substitution of alkyl for H causes more C_3 but less C_2 and C_4 intermediates. For cyclohexane, the fact that more C_2 and C_4 than C_3 are seen can be understood simply from the rule of β-scission. As shown in Figure 11, due to the special, symmetric structure of cyclohexane molecules, the cyclohexyl radical undergoes ring opening at only one possible position, the C-C bond next to the radical site, which produces CH_2=CH-CH_2-CH_2-CH_2-CH_2*. According to the β-scission rule, the radical CH_2=CH-CH_2-CH_2-CH_2-CH_2* also has only one option for further chain breaking because the radical site is at the end. This β-scission produces C_2H_4 and a C_2=CH-CH_2-CH_2*. As shown in the reaction path analysis by Ji *et al.* [7], beside further chain breaking the radical CH_2=CH-CH_2-CH_2-CH_2-CH_2* can also undergo radical site shifting, producing CH_2=CH-CH*-CH_2-CH_2-CH_3 radical. However, the new radical CH_2=CH-CH*-CH_2-CH_2-CH_3 also has only one option for further β-scission due to the presence of the double bond, which produces 1,3-C_4H_6 and C_2H_5*. We see that crack of cyclohexane clearly favors C_2 and C_4 over C_3 fragments under β-scission rule.

The initial cracking of methyl- and ethyl-cyclohexane, however, is more complicated than cyclohexane because the presence of alkyl breaks the symmetry and causes a branched carbon structure. Here we only look at the impact of ring opening positions on carbon structure of subsequent fragments, without considering the position of radical site and double bond formation. As shown in Figure 12, for methyl-cyclohexane there are three possible positions for ring opening, differentiated by the distance to the methyl group. Among the three, only when the ring is opened at the C-C bond next to methyl group, a straight-chain radical will be produced; the other two ways of ring opening will produce branched-chain radicals. Indeed, as shown in Figure 13 there are significantly more iso-butane and iso-butene (which are the main branched intermediates) in flames of methyl-cyclohexane than those of cyclohexane. The subsequent cracking of the branched-chain radicals produces various smaller fragments, leading to a more balanced distribution C_2-C_4 species as shown in Figure 10.

Additionally, species with branched structure themselves have been shown to have low reactivity thus slow flame propagation, such as the laminar flame speeds of iso-butane versus n-butane [4,20], iso-butanol versus n-butanol [26], and iso-octane versus n-octane [9,27]. This also helps to explain the lower flame speeds of alkylated cyclohexane relative to cyclohexane.

5. Concluding Remarks

Using expanding spherical flames, laminar flame speeds for cyclohexane, methylcyclohexane and ethyl-cyclohexane were measured at atmospheric and elevated pressures up to 20 atm, and unburned gas temperature of 353 K. The resulting data at atmospheric pressure show reasonably good agreement with the measurements of Ji *et al.* [7]. Predictions of JetSurf 2.0 mechanism yield satisfactory agreement with the present data for all three fuels at all pressures, with slight over-prediction at atmospheric pressure.

The present measurements show that the flame speeds of cyclohexane are uniformly higher than those of methyl-cyclohexane and ethyl-cyclohexane, thereby confirming the qualitative trend found by Ji et al. [7] at atmospheric pressure. Both predictions of JetSurf 2.0 mechanism and the present results at elevated pressures show that the difference in flame speeds for the three fuels increase from approximately 5% at 1 atm to 13% at 10 atm.

Examination of the computed flame structures indicated the effects of alkyl group substitution on flame propagation. Different from n-alkanes, which all crack into similar intermediate fragments in flames, cyclohexane cracks into substantially more chain-branching C_2 and C_4 fragments than the relatively less reactive C_3 fragments, owing to its special, symmetric ring structure and the general applicability of the β-scission rule. However, because of the alkyl substitution, methyl- and ethyl-cyclohexane crack into more balanced amount of C_2, C_3 and C_4 fragments, as well as relatively more intermediates with branched-chain structure, which have been shown to be less reactive compared to straight-chain molecules.

Acknowledgments

This research was supported by the Air Force Office of Scientific Research under the technical monitoring of Dr. Julian M. Tishkoff. It is a pleasure to acknowledge helpful discussions with Yuxuan Xin and Dr. Peng Zhang.

References

[1] W.J. Pitz, N.P. Cernansky, F.L. Dryer, F.N. Egolfopoulos, J.T. Farrell, D.G. Friend, in:, Society of Automotive Engineers, 2007, pp. 2007-01-0175.
[2] J.T. Farrell, N.P. Cernansky, F.L. Dryer, D.G. Friend, C.A. Hergart, C.K. Law, R.M. Mcdavid, C.J. Mueller, A.K. Patel, H. Pitsch, in:, Society of Automotive Engineers, 2007, pp. Paper 2007-01-0201.
[3] M. Colket, T. Edwards, S. Williams, N.P. Cernansky, D.L. Miller, F.N. Egolfopoulos, P. Lindstedt, K. Seshadri, F.L. Dryer, C.K. Law, D. Friend, D.B. Lenhert, H. Pitsch, A. Sarofim, M. Smooke, W. Tsang, in:, American Institute of Aeronautics and Astronautics, 2007, pp. Paper 2007-770.
[4] S.G. Davis, C.K. Law, Combustion Science and Technology 140 (1998) 427-449.
[5] J.T. Farrell, R.J. Johnston, I.P. Androulakis, in:, SAE Paper, 2004, pp. 2004-01-2936.
[6] T. Dubois, N. Chaumeix, C.-E. Paillard, Energy and Fuels 23 (2009) 2453-2466.
[7] C. Ji, E. Dames, B. Sirjean, H. Wang, F.N. Egolfopoulos, Proceedings of the Combustion Institute 33 (2011) 971-978.
[8] H. Wang, E. Dames, B. Sirjean, D.A. Sheen, R. Tangko, A. Violi, J.Y.W. Lai, F.N. Egolfopoulos, D.F. Davidson, R.K. Hanson, C.T. Bowman, C.K. Law, N.P. Cernansky, D.L. Miller, R.P. Lindstedt, University of Southern California (2010).
[9] A.P. Kelley, A.J. Smallbone, D.L. Zhu, C.K. Law, Proceedings of the Combustion Institute 33 (2011) 963-970.
[10] C. Ji, E. Dames, Y.L. Wang, H. Wang, F.N. Egolfopoulos, Combustion and Flame 157 (2010) 277-287.
[11] X. You, F.N. Egolfopoulos, H. Wang, Proceedings of the Combustion Institute 32 (2009) 403-410.
[12] A.P. Kelley, A.J. Smallbone, D.L. Zhu, C.K. Law, 6th U.S. National Combustion Meeting (2009).
[13] A.P. Kelley, J.K. Bechtold, C.K. Law, in:, 7th U.S. National Combustion Meeting, 2011.
[14] C.K. Wu, C.K. Law, Proceedings of the Combustion Institute (1984) 1941-1949.
[15] A.P. Kelley, C.K. Law, Combustion and Flame 156 (2009) 1844-1851.
[16] G.H. Markstein, Journal of the Aeronautical Sciences 18 (1951) 199-209.
[17] A.P. Kelley, G. Jomaas, C.K. Law, Combustion and Flame 156 (2009) 1006-1013.
[18] M.P. Burke, Z. Chen, Y. Ju, F.L. Dryer, Combustion and Flame 156 (2009) 771-779.
[19] Z. Chen, M.P. Burke, Y. Ju, Proceedings of the Combustion Institute 32 (2009) 1253-1260.
[20] A.P. Kelley, Dynamics of Expanding Flames, 2011.
[21] R.J. Kee, J.F. Grcar, M.D. Smooke, J.A. Miller, E. Meeks, Premix: A Fortran Program for Modeling Steady Laminar One-dimensional Premixed Flames. Sandia Report 85-8240., 1985.
[22] A.J. Smallbone, W. Liu, C. Law, X. You, H. Wang, Proceedings of the Combustion Institute 32 (2009) 1245-1252.
[23] K. Kumar, J.E. Freeh, C.J. Sung, Y. Huang, Journal of Propulsion and Power 23 (2007) 428-436.
[24] G. Jomaas, X.L. Zheng, D.L. Zhu, C.K. Law, Proceedings of the Combustion Institute 30 (2005) 193-200.
[25] F. Wu, A.P. Kelley, C. Tang, D.L. Zhu, C.K. Law, International Journal of Hydrogen Energy (2011) 1-10.
[26] W. Liu, A.P. Kelley, C.K. Law, Proceedings of the Combustion Institute 33 (2011) 995-1002.

[27] A.P. Kelley, W. Liu, Y.X. Xin, A.J. Smallbone, C.K. Law, Proceedings of the Combustion Institute 33 (2011) 501-508.